Backward-Time Lagrangian Stochastic Dispersion Models and Their Application to Estimate Gaseous Emissions

THOMAS K. FLESCH AND JOHN D. WILSON

Division of Meteorology, Department of Geography, University of Alberta, Edmonton, Alberta, Canada

EUGENE YEE

Defence Research Establishment Suffield, Medicine Hat, Alberta, Canada

(Manuscript received 3 February 1994, in final form 1 June 1994)

ABSTRACT

"Backward" Lagrangian stochastic models calculate an ensemble of fluid element (particle) trajectories that are distinguished by each passing through an observation point. As shown, they can be faster and more flexible in calculating short-range turbulent dispersion from surface area sources than "forward" models, which simulate trajectories emanating from a source. Using a backward model, one may catalog a set of "touchdown" points (where trajectories reflect off the ground) and vertical touchdown velocities w_0 of particles "on their way to" a sensor location. It is then trivial to deduce the average concentration resulting from a surface source using the touchdown catalog: by summing the reciprocal of w_0 for touchdowns occurring within the source boundary. An advantage of this methodology is that while forward model trajectories are linked to a specific source, backward trajectories have no such dependence. In horizontally homogeneous flow, a "library" of touchdown catalogs (for representative surface roughnesses and atmospheric stabilities) would allow concentration (at a given height) to be rapidly calculated at *any* location from *any* uniform surface source.

A "well-mixed" backward model is exploited to calculate the touchdown points of particles passing over a small plot on their way to an observation tower and it is shown how to use those data to estimate the plot emission rate from a single measurement of average concentration, wind speed, and wind direction on the tower. The method was evaluated using 36 field experiments. Predicted emission rates using the backward method agreed well with mass balance estimates.

1. Introduction

When we mimic turbulent dispersion by calculating an ensemble of fluid element (particle) trajectories with Lagrangian stochastic (LS) models (or random-flight models), it is conceptually natural to calculate "forward" trajectories emanating from a source and moving toward a sensor location (the observation point). However, forward LS models are computationally expensive. When predicting average concentration downwind of an area source, the vast majority of emitted particles widely miss the sensor location. Unless the "instrument" at that sensor location has a very large sampling volume (V_{sens}; necessarily $V_{sens} > 0$ to "catch" a particle), the majority of trajectories contribute to our knowledge of the average concentration only *indirectly*, as being the fraction of emitted particles not occupying V_{sens}. If the source dimensions are large, or if high spatial resolution is needed, a very onerous computation may be needed to reach a statistically accurate prediction. One wonders, Is there an advantage to calculating trajectories backward in time, from the sensor location to the source?

Starting with Durbin (1980), two-particle backward LS models have been used to investigate concentration *fluctuation* statistics (in ideal, nonatmospheric flows). For that purpose, the backward formulation has two advantages: first, that the effects of finite instrument volume can be obviated (or quantified), because backward trajectories *can* be permitted to coincide at a *point* (sensor location); and second, that correct statistics of the fluctuating *mixing ratio* of a tracer can be obtained, even though the model takes no account of the incompressibility constraint (false compressibility implies false concentration fluctuation; for a review see Thomson 1990).

The purpose of this paper is to show that, even for the mundane case of calculating single-particle trajectories, the backward approach has much to offer in terms of efficiency, simplicity, and flexibility. This is especially the case in calculating short-range dispersion from surface area or volume sources (e.g., the hazard due to a chemical spill, or fertilizer volatilization from agricultural fields). In particular, we will show that the

Corresponding author address: Dr. Thomas K. Flesch, Department of Geography, University of Alberta, Edmonton, Alberta, Canada T6G 2H4.

procedure of Wilson et al. (1982; 1983), which allows the emission rate Q (kg m^{-2} s^{-1}) from circular surface sources to be deduced from a *single* measurement of *average* concentration, can be generalized (most naturally, with the aid of a backward model) to encompass *any* shape of source.

In section 2 we briefly review the theory of LS models (especially, Thomson's 1987 "well-mixed condition"), derive the relationship between a given forward model and the equivalent backward model, and show how to derive average concentration at a sensor location from an ensemble of backward trajectories. Some readers might skip section 3, whereby using hypothetical experiments we demonstrate the greater computational efficiency of the backward model compared with the forward model. The culmination of our work is section 4, where we utilize a "touchdown catalog" to estimate the emission rate of volatile liquids from small rectangular plots and compare those estimates with mass flux balance estimates obtained in a field experiment.

2. Backward LS approach

There are two important questions to consider in formulating a backward LS approach to determine concentration: What is the proper form of the underlying LS trajectory model and how can concentration estimates be extracted from known backward trajectories? We will limit our consideration to uniform sustained area or volume sources, with particular attention to surface area sources.

a. LS model

1) FORWARD MODEL

The usual computational basis of forward LS models is a generalized Langevin equation, which follows from the assumption that particle position $\mathbf{x}$ ($x_1, x_2, x_3 = x, y, z$: along-wind, across-wind, and vertical coordinates) and velocity $\mathbf{u}$ ($u_1, u_2, u_3 = u, v, w$: along-wind, across-wind, and vertical velocities) evolve jointly as a Markov process:

$$du_i = a_i(\mathbf{x}, \mathbf{u}, t)dt + b_{i,j}(\mathbf{x}, \mathbf{u}, t)d\xi_j,$$
$$dx_i = u_i\,dt, \qquad (1)$$

where a_i and $b_{i,j}$ are functions of $(\mathbf{x}, \mathbf{u}, t)$, and $d\xi_j$ is a random increment selected from a Gaussian distribution having average 0 and variance dt (with $d\xi_i$, $d\xi_j$ independent if $i \neq j$). Once a_i and $b_{i,j}$ have been specified, it is straightforward to calculate the average concentration of a passive tracer due to a given source: Eq. (1) is discretized (see the appendix) and used to calculate an ensemble of particle trajectories emanating from the source, and a volume average concentration (sustained source) is determined from the residence time of the particles within a sensor volume V_{sens}.

Thomson (1987) recognized an essential constraint on the Langevin equation coefficients; namely, that the Eulerian velocity probability density function $g_a(\mathbf{x}, \mathbf{u}, t)$ must satisfy the Fokker–Planck equation (FPE) corresponding to Eq. (1):

$$\frac{\partial g_a}{\partial t} = -\frac{\partial}{\partial x_i}(u_i g_a) - \frac{\partial}{\partial u_i}[a_i(\mathbf{x}, \mathbf{u}, t)g_a] + \frac{\partial^2}{\partial u_i \partial u_j}[B_{i,j}(\mathbf{x}, \mathbf{u}, t)g_a], \qquad (2)$$

where $B_{i,j}$ denotes $b_{i,k}b_{j,k}/2$. Thomson called this constraint the "well-mixed condition." Unfortunately, Eq. (2) does not have a unique solution for multidimensional models (Thomson 1987; Sawford and Guest 1988; Flesch and Wilson 1992). Thomson gives a particular solution under the restriction that g_a is Gaussian and that $B_{i,j}$ is independent of $\mathbf{u}$:

$$a_i = -B_{i,j}(\mathbb{V}^{-1})_{j,k}(u_k - U_k) + \frac{\phi_i(\mathbf{x}, \mathbf{u}, t)}{g_a},$$
$$V_{i,j} = \overline{(u_i - U_i)(u_j - U_j)},$$
$$\frac{\phi_i}{g_a} = \frac{1}{2}\frac{\partial V_{i,l}}{\partial x_l} + \frac{\partial U_i}{\partial t} + U_l\frac{\partial U_i}{\partial x_l} + \left[\frac{1}{2}(\mathbb{V}^{-1})_{l,j}\left(\frac{\partial V_{i,l}}{\partial t} + U_m\frac{\partial V_{i,l}}{\partial x_m}\right) + \frac{\partial U_i}{\partial x_j}\right](u_j - U_j) + \frac{1}{2}(\mathbb{V}^{-1})_{l,j}\frac{\partial V_{i,l}}{\partial x_k}(u_j - U_j)(u_k - U_k). \qquad (3)$$

Here u_i is the instantaneous particle velocity, and U_i is the average velocity of the background flow. In this study, we have used

$$B_{i,j} = \delta_{i,j}\frac{\sigma_w^2}{\tau_l}, \quad \text{or} \quad b_{i,j} = \delta_{i,j}\left(\frac{2\sigma_w^2}{\tau_l}\right)^{1/2}, \qquad (4)$$

where σ_w^2 is the Eulerian vertical velocity variance, and τ_l is the Lagrangian decorrelation timescale for w. This familiar specification was used in the one-dimensional models of Thomson (1987) and Luhar and Britter (1989). Flesch and Wilson (1992) found that a two-dimensional model based on Eqs. (3) and (4) accurately predicted dispersion within the complicated flow of a crop canopy.

2) BACKWARD MODEL

Suppose an observer O tracks particles in the forward time frame, using coordinates $(\mathbf{x}, t)$ and sees particle velocity $u_i = dx_i/dt$. An observer O' tracks the same particles, but in a backward time frame. Observer O' shares the same position coordinate $(\mathbf{x})$ as O but uses time coordinate $t' = T_0 - t$, where T_0 is an arbitrary transformation constant (we will assume $T_0 = 0$). Particle velocity according to O' is then

$$u'_i = \frac{dx_i}{dt'} = \frac{dx_i}{-dt} = -u_i.$$

We can write a trajectory model for the evolution of particle velocity as seen in the coordinate system $(\mathbf{x}, \mathbf{u}', t')$ based on a generalized Langevin equation:

$$du'_i = a'_i(\mathbf{x}, \mathbf{u}', t')dt' + b'_{i,j}(\mathbf{x}, \mathbf{u}', t')d\xi_j,$$
$$dx_i = u'_i dt'. \quad (5)$$

The problem is to select the model coefficients a'_i and $b'_{i,j}$.

Consider the probability of a tracer particle traveling between $\mathbf{x}_1$ and $\mathbf{x}_2$. Observer O sees a conditional probability density $P^f(\mathbf{x}_2, \mathbf{u}_2, t_2|\mathbf{x}_1, \mathbf{u}_1, t_1)$, which is the probability that a particle moving forward from $(\mathbf{x}_1, \mathbf{u}_1)$ at an initial time t_1, will be found at $(\mathbf{x}_2, \mathbf{u}_2)$ at a later time t_2. Observer O' sees the same event but writes $P^b(\mathbf{x}_1, \mathbf{u}'_1, t'_1|\mathbf{x}_2, \mathbf{u}'_2, t'_2)$ for particles moving backward from $(\mathbf{x}_2, \mathbf{u}'_2, t'_2)$ to $(\mathbf{x}_1, \mathbf{u}'_1, t'_1)$. The evolution of P^b with t'_1 (for fixed $\mathbf{x}_2, \mathbf{u}'_2, t'_2$) is given by an FPE:

$$\frac{\partial P^b}{\partial t'_1} = -\frac{\partial}{\partial x_{1,i}}(u'_{1,i}P^b) - \frac{\partial}{\partial u'_{1,i}}[a'_i(\mathbf{x}_1, \mathbf{u}'_1, t'_1)P^b] + \frac{\partial^2}{\partial u'_{1,i}\partial u'_{1,j}}[B'_{i,j}(\mathbf{x}_1, \mathbf{u}'_1, t'_1)P^b].$$

A similar FPE is valid for the unconditional probability density function of the distribution of tracer particles in $(\mathbf{x}, \mathbf{u}')$ phase space, $g'(\mathbf{x}, \mathbf{u}', t')$ (Gardiner 1985):

$$\frac{\partial g'}{\partial t'} = -\frac{\partial}{\partial x_i}(u'_i g') - \frac{\partial}{\partial u'_i}(a'_i g') + \frac{\partial^2}{\partial u'_i \partial u'_j}(B'_{i,j}g').$$

If the tracer fluid elements are simply a subset of all fluid elements (from which we chose to follow those marked at $\mathbf{x}_2, t'_2$), we can substitute the Eulerian probability density function for all fluid elements, $g'_a(\mathbf{x}, \mathbf{u}', t')$, for g' in the FPE:

$$\frac{\partial g'_a}{\partial t'} = -\frac{\partial}{\partial x_i}(u'_i g'_a) - \frac{\partial}{\partial u'_i}(a'_i g'_a) + \frac{\partial^2}{\partial u'_i \partial u'_j}(B'_{i,j}g'_a).$$

This can be expressed in the $(\mathbf{x}, \mathbf{u}, t)$ coordinate system, noting that $g'_a(\mathbf{x}, -\mathbf{u}', -t') = g_a(\mathbf{x}, \mathbf{u}, t)$, $\mathbf{u}' = -\mathbf{u}$, and $\partial/\partial t' = -\partial/\partial t$:

$$\frac{\partial g_a}{\partial t} = -\frac{\partial}{\partial x_i}(u_i g_a) - \frac{\partial}{\partial u_i}(a'_i g_a) - \frac{\partial^2}{\partial u_i \partial u_j}(B'_{i,j}g_a), \quad (6)$$

where a'_i and $B'_{i,j}$ are evaluated at $(\mathbf{x}, -\mathbf{u}', -t') = (\mathbf{x}, \mathbf{u}, t)$. Requiring a'_i and $B'_{i,j}$ to satisfy this FPE results in a well-mixed backward model.

As Eq. (6) differs from Eq. (2) only in the sign of the last term on the right, we can easily obtain a particular solution a'_i by modifying the solution to Eq. (2) given by Eqs. (3),

$$a'_i = B'_{i,j}(\mathbf{V}^{-1})_{j,k}(u_k - U_k) + \frac{\phi_i}{g_a}(\mathbf{x}, \mathbf{u}, t). \quad (7)$$

As the magnitude of the random velocity fluctuations of fluid elements should be the same for both time frames, we choose $b'_{i,j} = b_{i,j}$ [Eq. (4)], and thus $B'_{i,j} = B_{i,j}$. The coefficient a'_i therefore differs from a_i only by a sign change on the first term on the right. This same result is obtained by Thomson (1987). Equations (4), (5), and (7) are the well-mixed backward trajectory model equivalent to the forward model of Eqs. (1), (3), and (4).

b. *Calculating average concentration*

1) FORWARD MODEL

The ensemble average tracer concentration at position $\mathbf{x}$ and time t, due to an arbitrary mass source density S (kg m^{-3} s^{-1}), can be written

$$C(\mathbf{x}, t) = \int_{-\infty}^{t}\int_{-\infty}^{\infty} S(\mathbf{x}_0, t_0)P^f(\mathbf{x}, t|\mathbf{x}_0, t_0)d\mathbf{x}_0 dt_0, \quad (8)$$

where $P^f(\mathbf{x}, t|\mathbf{x}_0, t_0)$ is the transition probability density, defined such that $P^f(\mathbf{x}, t|\mathbf{x}_0, t_0)\,d\mathbf{x}$ is the probability that a fluid element initially at $(\mathbf{x}_0, t_0)$ is found at time t in the volume $d\mathbf{x}$ centered on $\mathbf{x}$. The calculation of $P^f(\mathbf{x}, t|\mathbf{x}_0, t_0)$ is (in effect) the function of an LS model. Since we are concerned with a sustained source, whose emission rate is uniform over the source volume (or area), we may write

$$S(\mathbf{x}_0, t_0) = SW(\mathbf{x}_0),$$

where S is the tracer emission rate within the source volume and $W(\mathbf{x}_0)$ is a dimensionless localizing function (0 or 1) that vanishes outside the source. In stationary turbulence the average concentration (for a steady source) is time independent, and P^f depends upon $t - t_0$ (but not t or t_0 separately), so that

$$C(\mathbf{x}) = S\int_{t=0}^{\infty}\int_{\mathbf{x}_0=-\infty}^{\infty} W(\mathbf{x}_0)P^f(\mathbf{x}, t|\mathbf{x}_0, 0)d\mathbf{x}_0 dt.$$

In a forward LS model, what is calculated in practice is the concentration averaged over a "sensor" volume V_{sens}; that is,

$$C^v(\mathbf{x}) = \frac{S}{V_{\text{sens}}}\int_{V_{\text{sens}}}\int_{t=0}^{\infty}\int_{\mathbf{x}_0=-\infty}^{\infty} W(\mathbf{x}_0) \times P^f(\mathbf{x}, t|\mathbf{x}_0, 0)d\mathbf{x}_0 dt d\mathbf{x}.$$

The $C^v(\mathbf{x})$ is conveniently determined from the easily calculated ensemble-average particle "residence time" within V_{sens} (centered at $\mathbf{x}$) of particles released from $\mathbf{x}_0$,

$$\overline{T^f}(\mathbf{x}, V_{\text{sens}}|\mathbf{x}_0) = \int_{V_{\text{sens}}}\int_{t=0}^{\infty} P^f(\mathbf{x}', t|\mathbf{x}_0, 0)dt d\mathbf{x}', \quad (9)$$

so that

$$C^v(\mathbf{x}) = \frac{S}{V_{\text{sens}}} \int_{\mathbf{x}_0=-\infty}^{\infty} W(\mathbf{x}_0)\overline{T^f}(\mathbf{x}, V_{\text{sens}}|\mathbf{x}_0)d\mathbf{x}_0$$

$$= \frac{S}{V_{\text{sens}}} \int_{V_{\text{src}}} \overline{T^f}(\mathbf{x}, V_{\text{sens}}|\mathbf{x}_0)d\mathbf{x}_0, \quad (10)$$

where V_{src} denotes the volume occupied by the source. In practice $C^v(\mathbf{x})$ would be calculated from the average of a sample of individual particle residence times (stochastic variables),

$$C^v(\mathbf{x}) = S\frac{V_{\text{src}}}{V_{\text{sens}}}\frac{1}{N}\sum_{n=1}^{N} T_n^f(\mathbf{x}, V_{\text{sens}}|V_{\text{src}}),$$

where N particles are evenly released throughout V_{src}. For a sustained ground-level area source,

$$C^v(\mathbf{x}) = Q\frac{A_{\text{src}}}{V_{\text{sens}}}\frac{1}{N}\sum_{n=1}^{N} T_n^f(\mathbf{x}, V_{\text{sens}}|A_{\text{src}}),$$

where Q is the tracer emission rate from the surface (kg m^{-2} s^{-1}), A_{src} is the source area, and N particles are evenly released across A_{src}.

2) BACKWARD MODEL

A forward LS model is well suited to give predictions of concentration, through Eq. (8), because it naturally gives an estimation of the forward-time conditional probability density, $P^f(\mathbf{x}, t|\mathbf{x}_0, t_0)$, for particles released at $(\mathbf{x}_0, t_0)$ and collected at $(\mathbf{x}, t)$, with $t_0 < t$. In contrast, we envision a backward model where particles are released at $(\mathbf{x}, t)$ and collected at $(\mathbf{x}_0, t_0)$, giving an estimation of the backward-time conditional probability density $P^b(\mathbf{x}_0, t_0|\mathbf{x}, t)$.

(i) *Backward–forward probability equivalence*

Lundgren (1981) and Egbert and Baker (1984) show that for incompressible flow $P^f = P^b$. We can simply illustrate this from the multiplication law of probability. The probability that arbitrary events A and B both occur is

$$P(A \cap B) = P(A)P(B|A) = P(B)P(A|B),$$

where $P(A|B)$ is the probability of A occurring given the occurrence of B, $P(B|A)$ is the probability of B conditional on event A, and $P(A)$ and $P(B)$ are unconditional probabilities of A and B occurring, respectively. Therefore,

$$P(B|A) = \frac{P(B)}{P(A)}P(A|B).$$

From this general result, we equate the forward and backward probability of any given particle in the flow domain occupying $(\mathbf{x}_0, t_0)$ and $(\mathbf{x}, t)$:

$$P^b(\mathbf{x}_0, t_0|\mathbf{x}, t) = \frac{\rho_a(\mathbf{x}_0, t_0)}{\rho_a(\mathbf{x}, t)}P^f(\mathbf{x}, t|\mathbf{x}_0, t_0), \quad (11)$$

where $\rho_a(\mathbf{x}_0, t_0)$ and $\rho_a(\mathbf{x}, t)$ are the unconditional probability densities for fluid element occupancy of $(\mathbf{x}_0, t_0)$ and $(\mathbf{x}, t)$, respectively, that is, simply the marginal probability densities for position obtained from the joint density g_a,

$$\rho_a(\mathbf{x}, t) = \int_{-\infty}^{\infty} g_a(\mathbf{x}, \mathbf{u}, t)d\mathbf{u}.$$

As $\rho_a(\mathbf{x}, t)d\mathbf{x}$ is the probability of occupancy by any given fluid element in the volume $d\mathbf{x}$ centered on $\mathbf{x}$, $\rho_a(\mathbf{x}, t)$ is proportional to the air density at that point and time. If we restrict our attention to a stationary atmospheric boundary layer, we can assume incompressibility, and so $\rho_a(\mathbf{x}_0, t_0) = \rho_a(\mathbf{x}, t)$. Then

$$P^b(\mathbf{x}_0, t_0|\mathbf{x}, t) = P^f(\mathbf{x}, t|\mathbf{x}_0, t_0).$$

(ii) *Concentration calculation*

It is clear that P^b can be substituted for P^f in calculating concentration, but how is P^b estimated with a backward LS model? Consider emission from a source volume V_{src}. In a forward model, P^f is calculated from the ensemble average residence time within V_{sens} for particles released from V_{src}. Consider a corresponding backward model residence time: the time spent within V_{src} (centered at $\mathbf{x}_0$) by particles released from V_{sens} (and followed backward),

$$\overline{T^b}(\mathbf{x}_0, V_{\text{src}}|\mathbf{x}) = \int_{V_{\text{src}}}\int_{t'=0}^{\infty} P^b(\mathbf{x}', t'|\mathbf{x}, 0)dt'd\mathbf{x}', \quad (12)$$

where $t' = -t$. For a stationary atmosphere, the equivalence between P^b and P^f is such that,

$$\int_{t=0}^{\infty} P^f(\mathbf{x}', t|\mathbf{x}_0, 0)dt = \int_{t=0}^{\infty} P^b(\mathbf{x}_0, 0|\mathbf{x}', t)dt$$

$$= \int_{t'=0}^{\infty} P^b(\mathbf{x}_0, t'|\mathbf{x}', 0)dt',$$

so when comparing Eqs. (9) and (12), we see that

$$\int_{V_{\text{src}}} \overline{T^f}(\mathbf{x}, V_{\text{sens}}|\mathbf{x}_0)d\mathbf{x}_0 = \int_{V_{\text{sens}}} \overline{T^b}(\mathbf{x}_0, V_{\text{src}}|\mathbf{x})d\mathbf{x}.$$

If $V_{\text{src}} = V_{\text{sens}}$, then the forward residence time within V_{sens} (of particles released from V_{src}) equals the backward residence time within V_{src} (of particles released from V_{sens}). On first sight this may appear to confirm Smith's (1957) reciprocal theorem, which states that "concentration at $\mathbf{x}'$ due to a source at $\mathbf{x}''$, with the flow in the positive x direction, is equal to the concentration at $\mathbf{x}''$ due to an identical source at $\mathbf{x}'$ (i.e., $V_{\text{sens}} = V_{\text{src}}$) when the direction of the flow is reversed": in

an LS model, concentration is proportional to residence time. But in fact this proves the theorem wrong, since

$$\int_{V_{src}} \overline{T^f}(\mathbf{x}, V_{sens}|\mathbf{x}_0)d\mathbf{x}_0 = \int_{V_{sens}} \overline{T^b}(\mathbf{x}_0, V_{src}|\mathbf{x})d\mathbf{x} \neq \int_{V_{sens}} \overline{T^{f(-U)}}(\mathbf{x}_0, V_{src}|\mathbf{x})d\mathbf{x},$$

where $T^{f(-U)}$ denotes the forward model operating with the mean velocity field reversed. Backward model residence time differs from the corresponding residence time according to a "reversed" forward model (**U** reversed), as the two LS models are not identical (their a_i coefficients differ) unless $\phi_i = 0$. Thus Smith's reciprocal theorem does not apply in general and in particular for inhomogeneous turbulence.

Substituting the backward residence time into Eq. (10) gives C^v as

$$C^v(\mathbf{x}) = \frac{S}{V_{sens}} \int_{V_{sens}} \overline{T^b}(\mathbf{x}_0, V_{src}|\mathbf{x})d\mathbf{x},$$

or in practice as

$$C^v(\mathbf{x}) = S\frac{1}{N}\sum_{n=1}^{N} T_n^b(\mathbf{x}_0, V_{src}|\mathbf{x}),$$

where N particles are released evenly from V_{sens}, and T_n^b are individual particle residence times (stochastic variables).

The case of a surface-area source of strength Q (kg m^{-2} s^{-1}) is straightforward if we think of the source as a thin volume extending an infinitesimal height dz above the ground ($V_{src} = A_{src}dz$), with an equivalent volumetric emission rate $S = Q/dz$. For a particle that hits the ground within the source boundary with a vertical "touchdown" velocity w_0 (which is reversed upon impact), the contribution to T^b is simply $2dz/|w_0|$, provided the particle passes upward and downward through dz in one time step. Concentration is then

$$C^v(\mathbf{x}) = \frac{Q}{dz}\frac{1}{N}\sum\left|2\frac{dz}{w_0}\right| = \frac{Q}{N}\sum\left|\frac{2}{w_0}\right|, \quad (13)$$

where the summation refers to all touchdowns within the source. (The number of such touchdowns may be larger or smaller than N.) Calculating concentration is therefore simple: release particles evenly within V_{sens} using the backward LS model and sum the reciprocal of w_0 for all touchdowns within the source.

One advantage of a backward LS methodology is the ability to get point concentration estimates. Forward models by necessity estimate concentration averaged over V_{sens}, and the specification of V_{sens} involves tradeoffs between model speed and accuracy, and the spatial resolution of the estimated C field. In a backward model, particles are released from the sensor location, so when releasing particles at a sensor *point*, Eq. (13) gives a point estimate of C.

3. Backward model efficiency

We examined the efficiency of a backward (versus forward) LS model for a case of short-range dispersion from a hypothetical surface area source. We used the forward model corresponding to Eqs. (1), (3), and (4), and the equivalent backward model, Eqs. (4), (5), and (7). Details of the model discretization, the atmospheric statistics used in the models [U_i, $\overline{(u_i - U_i)(u_j - U_j)}$, τ_1], and particle release and reflection are given in the appendix. These are defensible atmospheric surface-layer models under the assumption of stationary, horizontally homogeneous, Gaussian turbulence. (For dispersion from ground releases over short distances, these assumptions are quite acceptable.)

a. Discretization and reflection errors

It is well known that improperly constructed LS models may have the defect of wrongly distributing dispersing particles in such a way that, even if those particles were initially well mixed, in time they become unmixed. Thanks to Thomson's (1987) well-mixed condition, we now have the means to devise models that are in principle (infinitesimal model time step Δt) immune to this problem. But Wilson and Flesch (1993) have shown that particle reflection (an ad hoc procedure to keep particles within the flow domain) can result in spurious particle density gradients near boundaries (i.e., the LS model acts to create $\partial\rho(\mathbf{x}, t)/\partial x_i \neq 0$, even as $t \to \infty$, where $\rho(\mathbf{x}, t)$ is the tracer density), leading to concentration prediction errors even in otherwise well-mixed models. In our surface-layer model, spurious density gradients occurred due to height gradients in the flow statistics (e.g., σ_w^2 or τ_1), in which case a discrete trajectory model only approximates the continuous Markov process of (idealized) particle motion. When coupled with particle reflection, this approximation resulted in a density gradient at the surface (see Wilson and Flesch 1993).

In our experience, errors of this nature have a limited impact on forward models, causing significant concentration prediction errors only very near reflecting boundaries. But the biased motion near boundaries that is symptomatic of models that are not well mixed (either due to insufficiently small Δt or illegitimate use of reflection) can lead to more significant problems in backward models. The backward model results we have presented require $P^b = P^f$, and Eq. (11) shows that these are identical only if both the backward and forward LS models have the property of implying the same tracer distribution at large time after release. If the backward model violates this requirement at ground, concentration prediction errors will occur throughout the domain when it is applied to surface sources.

The discretization error in our backward model becomes insignificant if Δt is kept small. Our approach was simply to reduce the time step sufficiently to render

any spurious concentration gradient negligible (by statistically comparing model results with various Δt). This resulted in what may seem an unduly small time step, $\Delta t = 0.025\tau_1$, where τ_1 is the Lagrangian timescale.

b. Computation time

Consider evaporation from a circular area source (perhaps representing a chemical spill, Fig. 1) having a radius of 20 m in short grass (roughness length $z_0 = 0.01$ m). Suppose a prediction of C is needed at height $z_m = 2$ m at three positions (fetches): the source center, 50 m directly downstream from the source center, and 300 m downstream. We estimated the computation time needed for the forward and backward models to provide a stable estimate of mean concentration C (i.e., standard error of the estimate reduced to 10% of the true average, determined from the forward model using a very large number of particles). We examined three atmospheric states: strongly stable (with Obukhov length $L = 10$ m), neutral ($L = \infty$), and strongly unstable ($L = -10$ m). With the forward model it was necessary to specify V_{sens}. We wanted V_{sens} small, so that C^v approximates the point estimate C, and we selected a vertically oriented cylinder 0.2 m in height, centered at $z = 2$ m, having a horizontal radius of 0.5 m (Fig. 1). This is a realistic choice for V_{sens}, as a larger radius cylinder gave $C^v < C$.

For the aforementioned scenarios, we found the backward model was about 50 times faster than the forward model (atmospheric stability did not change this value). This difference was due to the scale discrepancy between A_{src} and V_{sens}. As A_{src} increases, fewer particles are needed in the backward model, and more particles are needed in the forward model. Increasing V_{sens} decreases the number of particles needed in the forward model. The aforementioned examples clearly showed cases in which backward models are more efficient in predicting concentration than forward models: short-range dispersion from a substantial area source. We could similarly show that for long-range concentration predictions from a point source (effectively a very small A_{src}), a forward model would be more efficient. Between these limiting cases, the computational advantage (forward method vs backward) is unclear. For our purposes, the simplicity and flexibility of the backward approach in any case outweighs considerations of computational efficiency, which in view of steady increases in computer speed, are probably of little long-term relevance.

c. Prerunning a backward model

The independence of the required ensemble of backward trajectories, with respect to the source geometry, allows for the possibility of prerunning a backward model, and rapidly calculating C from archived data when an emission (with its unique geometry) occurs. For a sustained surface source, all information needed to estimate C is contained in the touchdown positions (x_0, y_0) and velocities (w_0). Figure 2a shows a stochastic set of touchdown points for those particles that will eventually pass through the sensor location at ($x = 80$ m, $y = -20$ m, $z = 2$ m). Each touchdown location has an associated w_0. This dataset represents a release of 5000 particles in neutral stratification, with $z_0 = 0.01$ m. Consider the elliptical surface source shown in Fig. 2a, centered at $x = y = 0$, emitting a tracer gas. With the touchdown catalog created in advance, C at (80, −20, 2 m) is quickly determined by summing the reciprocals of w_0 for touchdowns within the ellipse. The computation time for such a sorting program is negligible. If C is needed for a different source, the sorting program simply resamples those touchdowns occurring within this "new" source.

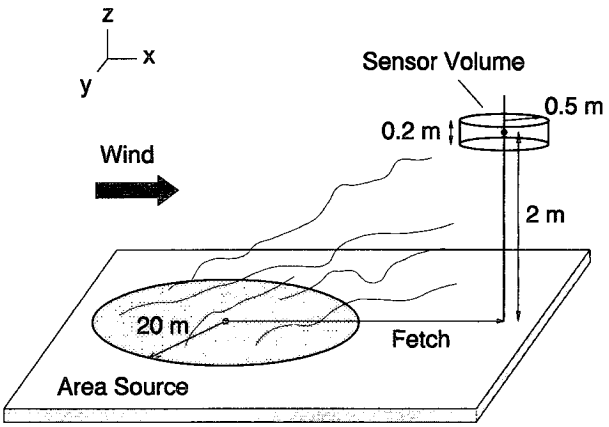

FIG. 1. Illustration of the source–sensor geometry used in the model computation time comparison. Concentration due to evaporation (of a neutrally buoyant gas) from a circular surface-area source was predicted with both forward and backward LS models. The forward model predicts the volume-averaged concentration within the "sensor volume," while the backward model estimates point concentration at the center of the sensor volume.

Because the velocity statistics in the LS model can be scaled on the friction velocity u_* (see the appendix), the touchdown field can be independent of average wind speed, and normalized concentration (u_*C/Q) is predicted. In uniform terrain, the touchdown field would also be independent of wind direction. Therefore, only a few archived touchdown catalogs (for different L and z_0 values) would be necessary to calculate C (at $z = 2$ m) for any surface area source in any atmospheric condition. A major advantage of the backward LS model is this ability to prerun the model without regard to the details of the eventual source geometry.

d. Multiple predictions

For horizontally homogeneous flow, the same touchdown data can be used to calculate C at multiple

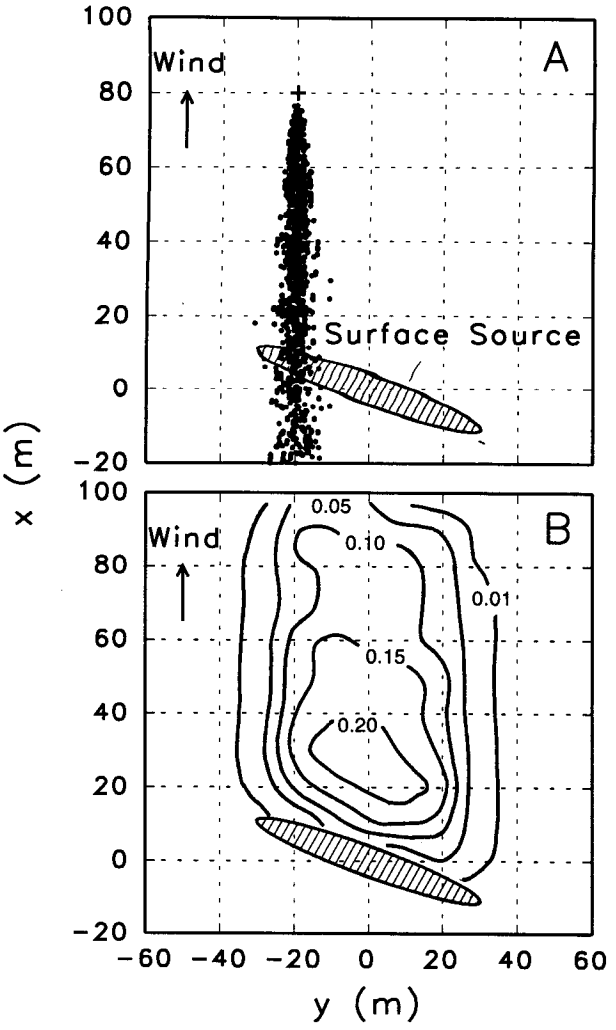

FIG. 2. (a) Catalog of the upstream touchdown positions of particles that will eventually pass through the location ($x = 80$, $y = -20$, $z = 2$ m) in neutral stratification, over a surface having $z_0 = 0.01$ m. The cross-hatched ellipse represents a surface source. (b) The normalized concentration field (Cu_*/Q) at $z = 2$ m due to the illustrated source in neutral stratification, obtained by repeated translation and resampling of touchdowns "within" the source.

locations (for a constant z_m). Figure 2a illustrates touchdown locations from which $C(80, -20, 2\text{ m})$ can be calculated. To calculate $C(60, 0, 2\text{ m})$, x_0 and y_0 are simply translated from the illustrated origin of (80, −20) to an origin of (60, 0), and this new set of touchdown points define C. Figure 2b shows the concentration field downstream of the elliptical surface source, determined by repeatedly translating and resampling the touchdown catalog to create a 10 m × 10 m grid of C estimates. Little computational effort was needed to create the 144 estimates: a single run of the backward model gave the touchdown catalog (5000 particles). Compare this with the 144 model runs that would be required by a forward model (each with tens of thousands of particle releases). We emphasize that the resampling of touchdowns to predict C at different locations requires horizontal homogeneity of the turbulence, a condition we generally assume when considering short-range dispersion in uniform terrain. Resampling would be valid for nonstationary turbulence, assuming changes in the flow occur over the whole domain at roughly the same time.

4. Estimating ground–atmosphere emission

A number of methods are available to estimate the emission rate Q from a ground surface: ground chamber measurements (e.g., Hutchinson and Mosier 1981), eddy correlation or flux gradient methods (see Stull 1988), eddy accumulation (e.g., Baker et al. 1992), the integrated horizontal flux method (e.g., Denmead et al. 1977), and dispersion model–based methods (e.g., Wilson et al. 1983). Each approach has advantages and disadvantages, and each can be effective (see review by Denmead and Raupach 1993). But in terms of accuracy, simplicity of instrumentation, applicability to arbitrary source geometry, and suitability for any chemical species, the dispersion-based methodology is often superior. This method, in a form applicable only to circular sources, is described by Wilson et al. (1982, 1983). We will show how this method can be conveniently generalized to plots of any shape, using a backward LS model.

a. Dispersion model–based methodology

Assume a horizontally uniform surface source and an atmosphere in horizontal equilibrium. (Throughout this paper we have neglected the complications that arise if a full plant canopy is present.) The average horizontal wind speed U (m s^{-1}) and concentration C (kg m^{-3}) observed at any height z_m are known to satisfy

$$\frac{UC}{Q} = n = f(z_m, z_0, L, h, G),$$

where L is the Obukhov stability length, h is the depth of the mixed layer (which has but a slight influence in the case of short-range dispersion), and G denotes the set of variables characterizing the source: its shape and outline, orientation with respect to the wind, and its position with respect to the location where U and C are observed. We see at once that, if n is determined, then a measurement of U and C determines Q.

One can determine n using a turbulent dispersion model. The practical advantages of such an approach are important: only one observation of U and C is necessary, and slow response sensors can be used (in contrast to eddy correlation). If the source geometry is correctly accounted for in the dispersion model, there are no limitations on selecting a measurement site (i.e., no requirement for a large fetch of source area), and it would be unnecessary to erect a substantial tower.

The success of this method depends upon using an accurate dispersion model that will allow incorporation of the complexities of the source geometry. (Of course any assumptions implicit in the model, such as horizontal flow uniformity, must be upheld at the actual site.) The backward LS model presented in this paper is well suited for this task.

b. *Procedure for estimating Q with a backward LS model*

Predicting n from a set of backward trajectories is straightforward. By normalizing the touchdown velocities in the LS model by $U(z_m)$, the height z_m is selected as a matter of convenience prior to the trajectory calculations, then Eq. (13) can be rewritten as

$$n(z_m) = \frac{C(z_m)U(z_m)}{Q} = \frac{1}{N}\sum\left|\frac{2}{w_0/U(z_m)}\right|, \quad (14)$$

where the summation refers to touchdowns occurring within the source boundary. The constant n is dependent upon z_m, z_0, L, and h through the LS model, and on G through a sampling program that selects the touchdown locations within the source. The use of a backward LS model to calculate n represents an improvement over the methodology used by Wilson et al. (1982; 1983). By basing the calculation on a backward trajectory touchdown catalog, n can be rapidly and easily determined for any location in, or downstream from, an arbitrary surface source—not just from observations at the center of a necessarily circular plot.

Our new procedure for estimating Q has three steps: 1) run a backward LS model and catalog the touchdowns; 2) make on-site measurements of C, U, and wind direction; and 3) use a sampling program to match the touchdowns with the geometry of the source, calculating n with Eq. (14). One of the advantages of the backward model is the ability to prerun the LS model, creating a touchdown catalog without any knowledge of the source geometry. Then when a source occurs, a tower is placed at z_m within, or downstream of, the source to measure C, U, and wind direction. (The term "tower" is used generically to indicate the instrument assembly.) A cup anemometer and a slow-response concentration sensor would be preferable for this purpose (the underlying LS model of atmospheric dispersion is valid only in a time-averaged sense, and so the on-site observations of U and C must also correspond to time-averaged values). The final step is to estimate n by using a sampling program to overlay the source geometry onto the field of touchdown points.

It is worth emphasizing the assumptions invoked in the methodology: a spatially uniform emission rate and horizontally homogeneous flow. Of course no situation will meet these criteria in detail, and some error in the estimate of Q will result. But in many cases, such errors can be kept small. Horizontal homogeneity is of critical importance for our method, which relies on the independence of the touchdown catalogs with respect to sensor location and wind direction. In complex terrain, such as flow through a valley, the inhomogeneity may be on relatively large scale, and the method valid if the fetch is kept small (and the local flow accurately parameterized in the LS model). At the other extreme, an area source may be bare soil surrounded by short grass, with inhomogeneity introduced by the step change in surface roughness. But this inhomogeneity will be of little importance if the source dimensions and the sensor height are kept large in relation to the roughness heights. To better determine the spatial average of Q when the emission rate varies, sensors should be placed as far downwind of the source as possible (while still having a detectable C level). This both increases the effective sampling area and gives a more even spatial "weighting" over the source (touchdowns more evenly spread). Any information on the spatial variability of Q within the source requires measurements of C at different locations. Likewise, if two sources contribute to create a joint plume, C measurements at two locations would be needed to determine Q for each source (three C measurements for three sources, etc.). In principle, these two measurements need only be slightly separated.

c. *Validation of the backward LS methodology*

The backward LS methodology for estimating Q was evaluated using emission data from 36 field experiments, conducted in near-neutral conditions at the Experimental Proving Ground of the Defence Research Establishment Suffield, in southern Alberta, Canada. The short-grass prairie terrain was uniformly flat with $z_0 \approx 0.025$ m. A summary of the major characteristics of the experiments is presented in Table 1. Four series of experiments were conducted, each designed to document the time dependence of the emission rate $Q(t)$ for a specific volatile chemical, namely, dipropylene glycol methyl ether (DPM), triethylphosphate (TEP), dimethyl sulfoxide (DMSO), and methyl salicylate (MS). The chemicals were spread over a rectangular surface plot using either of two methods: 1) an explosive dissemination from polypropylene bottles suspended 1 m above the surface to produce a contaminated source of 24 m (across wind) by 16 m (along wind), or 48 m (across wind) by 16 m (along wind); or 2) a modified agricultural sprayer that created a source 100 m (across wind) by 25 m (along wind).

An estimated emission rate was obtained for each experiment by the mass balance approach. Integrating the time-averaged along-wind vapor flux measured by average concentration and wind speed sensors in a vertical sampling array, we have

$$Q_m = \frac{1}{D}\int_0^\infty C(z)U(z)dz, \quad (15)$$

where D is the along-wind source length. Concentration was determined from vapor dosages measured using

bubblers analyzed by liquid chromatography, and wind speed was measured using cup anemometers. For the TEP, DMSO, and MS experiments, three sampling arrays (with sensors at z = 0.3, 0.5, 1.0, and 1.5 m) were placed at the downwind edge of the source (at the across-wind midpoint and 3 m either side of the midpoint), and Q_m was averaged over the arrays. For the DPM experiments, one array (sensors at z = 0.5, 1.0, 2.0, 3.0, and 4.0 m) was deployed 5 m downwind of the downwind plot edge, at the across-wind midpoint. In each experiment, Q_m was measured over the various sampling intervals indicated in Table 1, ranging from 0–3 min to 210–300 min after release. It should be emphasized that Q_m is an imperfect estimate of the true flux Q. One reason for this is that measurements were not available for vapor fluxes above and below the highest and lowest samplers. Consequently, the low- and high-level fluxes were not known and were assumed to be zero. Another flaw in Q_m is that Eq. (15) neglects the turbulent part of the along-wind flux of material past the sensor array.

We calculated an estimate of Q_b for each measurement of Q_m, using the backward LS scheme we have described. We used a neutral stratification surface-layer LS model, based on Eqs. (4), (5), and (7), as outlined in the appendix. We created a single touchdown catalog from 15 000 particle releases, oriented this catalog with respect to the source geometry, and calculated n at z_m = 1 m for each experiment. The Q_b was then determined from $C(z_m)$ and $U(z_m)$. The backward LS methodology has less accuracy over the shorter sampling intervals used in these trials. The LS model is valid only in a time-averaged sense (the ensemble of trajectories are representative of expected conditions over a nominal averaging period of order 15 min or more), and so the on-site observations of U and C should correspond to at least 15 min of measurements. Regardless, we have included Q_b calculated for time intervals less than 15 min.

Figure 3 shows the temporal evolution of Q_m taken from one MS trial. As expected, the evaporative flux

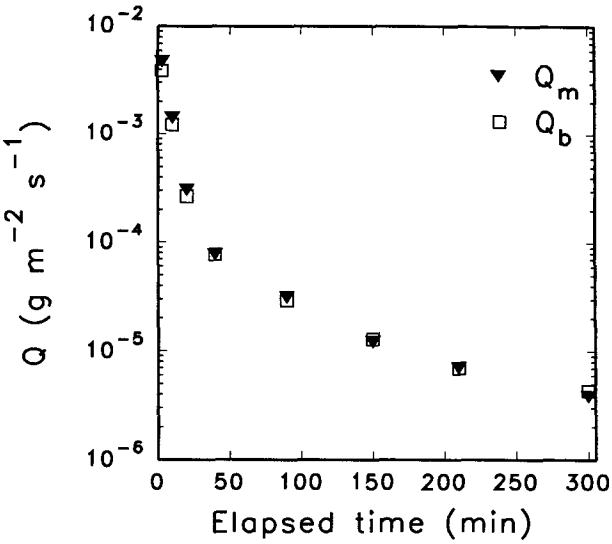

FIG. 3. Time evolution of the surface emission rate (Q) as estimated by a mass flux balance (Q_m) and the backward LS model methodology (Q_b), for one of the MS field trials.

decreased with time, and it can be seen that Q_b tracked the time development of Q_m quite well. In this example, Q_b initially was smaller than Q_m, but this negative bias disappeared as the emission from the source progressed. The Q_b bias at the early times, where the estimates were short interval averages, may have been due to an inadequate averaging time.

Figure 4 compares Q_m and Q_b for the MS and DMSO experiments. Visually, the agreement was very good, and this extended to the TEP and DPM experiments as well. There appeared to be a slight tendency for overprediction in Q_b in the DMSO experiment, and an underprediction in the MS experiments. It is surprising that there seemed to be no decrease in Q_b accuracy for the shorter time intervals of the experiment. We evaluated the quantitative agreement between the two estimates using the fractional bias (FB) and normalized mean-square error (NMSE):

TABLE 1. Summary of the emission experiments conducted at the Defence Research Establishment Suffield in southern Alberta, under near-neutral stability, at a uniformly flat short-grass prairie site ($z_0 \approx 0.025$ m).

Chemical material	DPM	TEP	DMSO	MS
Number of trials	7	8	12	9
Type of release	Sprayer	Explosive	Explosive	Explosive
Plot area	100 m × 25 m	24 m × 16 m	24 m × 16 m	24 m × 16 m 48 m × 16 m
Surface contamination density (g m^{-2})	2.5	2.0	2.0	2.0
Vapor sampling schedule (interval in minutes, from the moment of release, over which concentration was averaged)	0–5 5–10 10–15 15–30 30–45	0–5 5–15 15–30 30–90 90–180	0–1 1–2 2–5 5–10 10–30 30–90 90–150	0–3 3–10 10–20 20–40 40–90 90–150 150–210 210–300

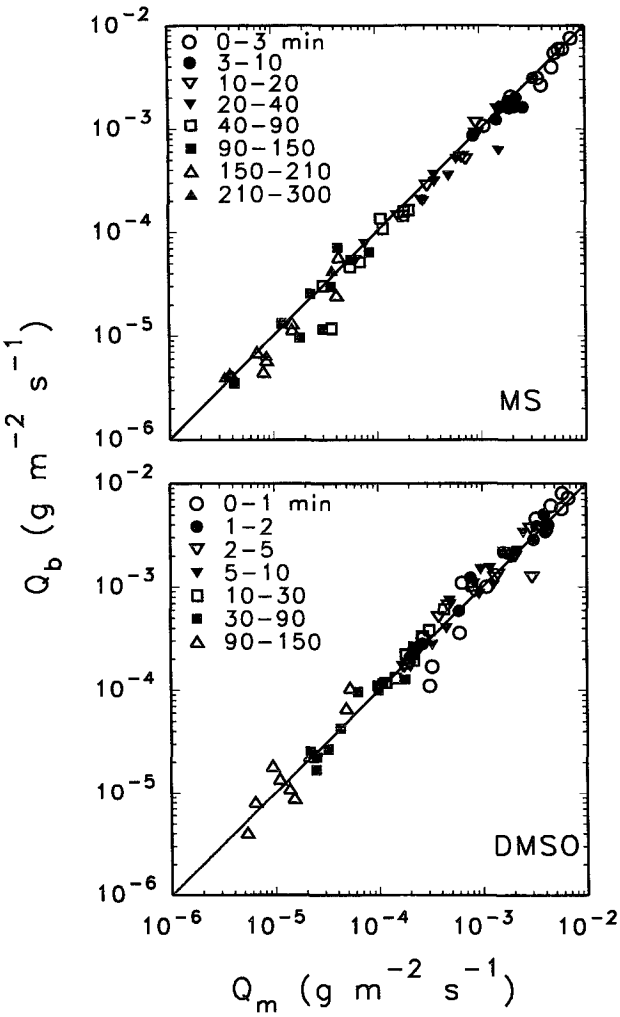

FIG. 4. Comparison of the mass flux balance estimate of the emission rate (Q_m) with the backward LS model-based estimate (Q_b) for the DPM and DMSO field trials, estimated at the indicated intervals after initial surface contamination.

$$\text{FB} = \frac{\overline{Q_b} - \overline{Q_m}}{0.5(\overline{Q_b} + \overline{Q_m})}, \quad \text{NMSE} = \frac{\overline{(Q_b - Q_m)^2}}{\overline{Q_b}\,\overline{Q_m}}.$$

Table 2 summarizes the calculated values of FB, NMSE, and the correlation coefficient r for each series of field trials as well as for all field trials considered as an entity. The 95% confidence limits on FB and NMSE are based on the 2.5% and 97.5% points of the bootstrap cumulative distribution function for these statistics (Hanna 1989).

The backward model-based estimates Q_b were negatively biased relative to the measured flux rates Q_m for the DPM and MS experiments, and positively biased in the TEP and DMSO experiments. The fractional bias ranged from −0.098 for the DPM field trials (indicating an underprediction of 9.8%) to 0.101 for the TEP trials (implying an overprediction of 10.1%), with an overall bias of 0.015 for all the trials. The bias in the DPM and TEP trials were not significantly different from zero at the 95% confidence level (i.e., Q_b was an unbiased estimate of Q_m in those trials). A linear least-squares regression of Q_b on Q_m using all the field trial data yielded $Q_b = (1.04 \pm 0.02)Q_m + (-0.000023 \pm 0.000029)$, with $r = 0.975$. The random scatter in the residuals between Q_b and Q_m as characterized by the NMSE was low—it ranged from 0.189 for the TEP trials to 0.031 for the DPM trials, with an NMSE for all trials of 0.139 (i.e., the statistical scatter in the differences between Q_b and Q_m is less than 20% for all runs). These results show that the backward LS method can be used to predict Q with a maximum mean bias of about 10% (although the overall bias was less than 2%) accompanied with a scatter in the prediction residual errors of 20% or less.

5. Summary and conclusions

Backward trajectory models have often been used, on the synoptic scale, to calculate the "origin" of a certain mass of (polluted?) air. The notion is simply to advect in the time-varying, large-scale horizontal velocity field, a loosely defined column of air that remains well mixed in the vertical. The distinction between forward and backward models of that type is trivial.

But the distinction is not so trivial, in the case of calculating *fluid element* trajectories in turbulence. To each forward Lagrangian stochastic (LS) trajectory model, which since Thomson (1987) will normally have been chosen to satisfy the well-mixed condition,

TABLE 2. Statistical evaluation of the agreement between the mass flux balance estimate of the emission rate (Q_m) and the backward LS model estimate (Q_b) for the 36 emission rate experiments.

Material	DPM	TEP	DMSO	MS	All
Number of observations	20	40	81	66	207
FB	−0.0983	0.101	0.0979	−0.101	0.0154
[95% conf. int.]	[−0.26, 0.025]	[−0.021, 0.20]	[0.013, 0.17]	[−0.18, −0.034]	[−0.038, 0.065]
NMSE	0.0313	0.189	0.172	0.0735	0.139
[95% conf. int.]	[0.015, 0.14]	[0.047, 0.34]	[0.064, 0.27]	[0.029, 0.20]	[0.082, 0.19]
r	0.995	0.982	0.968	0.988	0.974

there corresponds a backward model. We have reexamined the relationship between those models. The formalism tends to be more confusing than the fact: in backward trajectories, one must not fail to reverse the direction of any deterministic bias to the direction of motion, of the sort arising due to turbulence inhomogeneity (see Thomson 1987). We also examined one means to estimate the concentration due to a given source: focusing on the residence time of trajectories within some sensor volume.

There is often a considerable gain in computational efficiency to be had by using a backward model. But more significantly, in many dispersion problems the bulk of the calculations can be done without reference to the details of the eventual source! This permits adopting the LS method even where very rapid estimates of concentration due to a given source are needed (e.g., emergency response).

We have given a new means to estimate the emission rate Q from a sustained surface area source (of any shape) in horizontally homogeneous turbulence. In addition to an archive of backward trajectory touchdown points (and velocities), one requires only a measurement of the mean concentration of the species of interest, the mean horizontal wind speed, and the wind direction—these data taken at any location within, or downwind of, the source. The procedure is fast, requires only the simplest measurements, and applies to any shape of source. We have proven our method accurate, for rectangular plots in the case that the required measurements were taken close downwind in near-neutral stability. It remains to examine how robust the technique is with regard to less central positioning of the reference measurements (concentration and wind speed) in the emitted plume and in nonneutral conditions.

In applying our backward LS method, we have dealt exclusively with sustained surface sources. But the emission from instantaneous or transient sources might also be estimated, working either from instantaneous measured concentration, or for greater accuracy, a time series $C(t)$. In either case, touchdown *times* would also be recorded: source strength Q would be calculated by summing those touchdowns that occurred, within the source, within a time window about the instant (or period) when the source was active. (Of course if Q was so-estimated from only one realization, sampling variation about the true value would be inevitable.)

APPENDIX

LS Model Details

a. Discretization of the LS trajectory model

Discretization of the forward and backward trajectory models [Eqs. (1) or (5)] is necessary for their application. In many cases, model results are relatively insensitive to errors introduced by discretization, and so the details of discretization are unimportant (as long as the model time step is reasonably small, say $\Delta t < 0.2\tau_1$). But this is not the case when predicting dispersion from surface sources using a backward LS model. The location of the source at a reflecting boundary (ground) results in heightened sensitivity to discretization errors (as discussed in section 3a) and raises the importance of the discretization scheme.

Consider the backward trajectory model [Eqs. (5)] in stationary conditions. This model is made up of a stochastic differential equation for $\mathbf{u}'$ (Langevin equation):

$$du_i' = a_i'(\mathbf{x}, \mathbf{u}')dt' + b_{i,j}'(\mathbf{x})d\xi_j,$$

and the deterministic differential equation for $\mathbf{x}$,

$$dx_i = u_i' dt'.$$

The simplest discretization of this model would be an explicit Euler scheme, so that

$$(u_i')_{N+1} = (u_i')_N + a_i'(\mathbf{x}_N, \mathbf{u}_N')\Delta t' + b_{i,j}'(\mathbf{x}_N)\Delta\xi_j,$$

$$(x_i)_{N+1} = (x_i)_N + (u_i')_N\Delta t',$$

where the subscript N refers to model time-step number. This scheme is correct to order $\Delta t^{1/2}$ for $\mathbf{u}$ and Δt for $\mathbf{x}$ (Kloeden and Platen 1992). We found this scheme unsatisfactory in practice, as it led to an overestimation of concentration for a surface source, due to an anomalous particle density at the ground. Even decreasing the model time step to a very small $\Delta t' = 0.001\tau_1$ did not yield agreement with forward model results (which in this case are insensitive to discretization). More successful was an implicit scheme for $\mathbf{x}$ (using the explicit scheme for $\mathbf{u}'$),

$$(u_i')_{N+1} = (u_i')_N + a_i'(\mathbf{x}_N, \mathbf{u}_N')\Delta t' + b_{i,j}'(\mathbf{x}_N)\Delta\xi_j,$$

$$(x_i)_{N+1} = (x_i)_N + (u_i')_{N+1}\Delta t',$$

which had a much lower sensitivity to $\Delta t'$ than the explicit approach. We found good agreement with forward models when using this scheme with a time step $\Delta t' = 0.025\tau_l$, and the results given in this paper are based upon this discretization.

b. Wind flow parameterization

For a Gaussian turbulence LS model, it is necessary to prescribe U_i (average velocities), $\overline{(u_i - U_i)(u_j - U_j)}$ (velocity covariances), and τ_l (Lagrangian timescale). We selected functional forms valid for the surface layer, which require three surface-layer parameters: u_*, L, and z_0 (assuming that mixed-layer depth $h = 1000$ m in unstable conditions). This Gaussian model cannot account for the effects of skewness, which are important in larger-scale dispersion in the unstable boundary layer.

1) AVERAGE WIND VELOCITY PROFILE

Aligning x with the mean surface wind ensures $V = W = 0$. We specified U as

$$U = \frac{u_*}{k}\left[\ln\left(\frac{z}{z_0}\right) + \psi\left(\frac{z}{L}\right)\right].$$

Here k is von Kármán's constant, ψ is the Monin–Obukhov universal function, and L is the Obukhov length

$$L = -\frac{u_*^3\overline{\theta_v}}{kgH},$$

where θ_v is the virtual temperature and H is the kinematic surface heat flux. We specified ψ as (Businger et al. 1971; Paulson 1970):

$$\psi = \begin{cases} \dfrac{4.7z}{L}, & L > 0, \\ -2\ln\left(\dfrac{1+x}{2}\right) - \ln\left(\dfrac{1+x^2}{2}\right) \\ \qquad + 2\tan^{-1}(x) - \dfrac{\pi}{2} & L < 0, \end{cases}$$

where $x = (1 - 15z/L)^{0.25}$.

Our specification of $U(z)$ is slightly wrong, as the aforementioned formula is "calibrated for" and normally applied to, the "cup" wind speed

$$S = \overline{(u^2 + v^2)^{1/2}} \quad (>U),$$

so that S exceeds U, particularly near ground, where the horizontal velocity variances are relatively large compared to U. However, the distinction is small above about $5z_0$.

2) VELOCITY VARIANCES

The along-wind, across-wind, and vertical velocity variance are denoted σ_u^2, σ_v^2, and σ_w^2. We assume that the velocity covariances $\overline{(u-U)(v-V)}$ and $\overline{(v-V)(w-W)}$ vanish in the surface layer, and the value of $\overline{(u-U)(w-W)}$ is constant, equal to $-u_*^2$.

(i) *Stable and neutral stratification*

We created height-independent surface-layer formulas based on the profiles of Wyngaard et al. (1974), Hanna (1982), and Gryning et al. (1987), by assuming z/h is zero (as particles of interest will never reach large height):

$$\sigma_u^2 = 4.0u_*^2, \quad \sigma_v^2 = 2u_*^2, \quad \sigma_w^2 = 1.7u_*^2.$$

This height independence is only an approximation, as the variances do exhibit height variation, particularly very near the ground. However, Wilson et al. (1981) showed very accurate prediction of short-range dispersion in an LS model with a constant σ_w^2. We compared predictions of a model using the aforementioned parameterizations with a model using more accurate height-dependent values and found no significant difference between the two predictions for short-range dispersion (<1 km) from a surface source.

(ii) *Unstable stratification*

The variance of w in unstable conditions is height dependent in the surface layer, and we used the following formula from Panofsky et al. (1977):

$$\sigma_w^2 = u_*^2\left(2.2 - 6.6\frac{z}{L}\right)^{0.67}.$$

We assumed that $\sigma_u^2 = \sigma_v^2$ (roughly supported by observation) and used the formula for σ_v^2 given by Gryning et al. (1987), with $z/h = 0$. Thus,

$$\sigma_u^2 = \sigma_v^2 = 0.35w_*^2 + 2.0u_*^2,$$

where w_* is the convective velocity scale,

$$w_* = \left(\frac{ghH}{\overline{\theta_v}}\right)^{1/3} = \left(-\frac{u_*^3 h}{Lk}\right)^{1/3}.$$

Over short ranges, h significantly effects dispersion only through its effect on σ_v^2. (The effect of h on along-wind dispersion is limited in most cases as σ_u/U is small, and the effect of h in limiting vertical dilution is unimportant at short distances.) At a maximum sensitivity, σ_v^2 is proportional to $h^{0.67}$; so that overestimating h by a factor of 3 leads to an overestimation of σ_v^2 by roughly a factor of 2, and of lateral spread of a plume ($\sigma_y \propto \sigma_v$) by about 1.4. This relative insensitivity of short-range dispersion to h permits us to specify a constant value of h (chosen as 1000 m) in unstable conditions.

3) LAGRANGIAN TIMESCALE

We used the same decorrelation timescale for each of the three velocity components, from the formulas of Wilson et al. (1981), which were stability corrected in a rational manner and yielded agreement with the Project Prairie Grass short-range dispersion experiments:

$$\tau_l = \begin{cases} \dfrac{0.5z}{\sigma_w}\left(\dfrac{1}{1+5z/L}\right), & \text{for} \quad L > 0, \\ \dfrac{0.5z}{\sigma_w}\left(1 - 6\dfrac{z}{L}\right)^{0.25}, & \text{for} \quad L < 0. \end{cases}$$

These formula are equivalent for neutral stability ($|L| = \infty$). The selection of a single timescale for all velocity components is usually justifiable for short-range dispersion, where meso- and synoptic-scale fluctuations, with different component timescales, have little effect on dispersion.

c. *Particle release and reflection*

In the forward model, particles were released with random position distributed uniformly across the source at $z = z_0$, with a random velocity chosen from the Eulerian probability density distribution $g_a(z_0, \mathbf{u})$. In our backward model, particles were released at the sensor location of interest (x_m, y_m, z_m), with a randomly chosen velocity $\mathbf{u}' = -\mathbf{u}$, consistent with $g_a(z_m, \mathbf{u})$. The model time step Δt was chosen as $0.025\tau_l$, on the basis of trials to determine the largest Δt which still allowed only a negligible density buildup at the ground (by "density buildup," we mean a particle spatial distribution that was not perfectly uniform along the z axis).

The ground surface in the model was set at z_0 and taken to be a perfect reflector. When a particle reached the surface it was "bounced," and the sign of the along-wind and vertical velocity fluctuations [$(u - U)$ and w] were reversed (to retain proper u–w correlation). When a particle reached z_0 (touchdown), its horizontal position and vertical velocity [normalized by either u_* or $U(z_m)$ depending on the application] were recorded.

REFERENCES

Baker, J. M., J. M. Norman, and W. L. Bland, 1992: Field-scale application of flux measurement by conditional sampling. *Agric. For. Meteorol.*, **62,** 31–52.

Businger, J. A., J. C. Wyngaard, Y. Izumi, and E. F. Bradley, 1971: Flux-profile relationships in the atmospheric surface layer. *J. Atmos. Sci.*, **28,** 181–189.

Denmead, O. T., and M. R. Raupach, 1993: Methods for measuring atmospheric gas transport in agricultural and forest systems. *Agricultural Ecosystem Effects on Trace Gases and Global Climate Change,* ASA Special Publication No. 55, American Society of Agronomy, Madison, Wisconsin, 19–43.

——, J. R. Simpson, and J. R. Freney, 1977: A direct field measurement of ammonia emission after injection of anhydrous ammonia. *Soil Sci. Soc. Amer. J.*, **41,** 1001–1004.

Durbin, P. A., 1980: A stochastic model of two-particle dispersion and concentration fluctuations in homogeneous turbulence. *J. Fluid Mech.*, **100,** 279–302.

Egbert, G. D., and M. B. Baker, 1984: Comments on paper "The effect of Gaussian particle-pair distribution functions in the statistical theory of concentration fluctuations in homogeneous turbulence" by B. L. Sawford. *Quart. J. Roy. Meteor. Soc.*, **109,** 339–353. *Quart. J. Roy. Meteor. Soc.*, **110,** 1195–1199.

Flesch, T. K., and J. D. Wilson, 1992: A two-dimensional trajectory-simulation model for non-Gaussian, inhomogeneous turbulence within plant canopies. *Bound.-Layer Meteor.*, **61,** 349–374.

Gardiner, C. W., 1985: *Handbook of Stochastic Methods for Physics, Chemistry, and the Natural Sciences.* Springer-Verlag, 442 pp.

Gryning, S. E., A. A. M. Holtslag, J. S. Irwin, and B. Sivertsen, 1987: Applied dispersion modelling based on meteorological scaling parameters. *Atmos. Environ.*, **21,** 79–89.

Hanna, S. R., 1982: Applications in air pollution modelling. *Atmospheric Turbulence and Air Pollution Modelling,* F. T. M. Nieuwstadt and H. van Dop, Eds., Reidel Publishing, 275–310.

——, 1989: Confidence limits for air quality model evaluations, as estimated by bootstrap and jackknife resampling methods. *Atmos. Environ.*, **23,** 1385–1398.

Hutchinson, G. L., and A. R. Mosier, 1981: Improved soil cover method for field measurement of nitrous oxide fluxes. *Soil Sci. Soc. Amer. J.*, **45,** 311–316.

Kloeden, P. E., and E. Platen, 1992: Higher-order implicit strong numerical schemes for stochastic differential equations. *J. Stat. Phys.*, **66,** 283–314.

Luhar, A. K., and R. E. Britter, 1989: A random walk model for dispersion in inhomogeneous turbulence in a convective boundary layer. *Atmos. Environ.*, **23,** 1911–1924.

Lundgren, T. S., 1981: Turbulent pair dispersion and scalar diffusion. *J. Fluid Mech.*, **111,** 27–57.

Panofsky, H. A., H. Tennekes, D. H. Lenschow, and J. C. Wyngaard, 1977: The characteristics of turbulent velocity components in the surface layer under convective conditions. *Bound.-Layer Meteor.*, **11,** 355–361.

Paulson, C. A., 1970: The mathematical representation of wind speed and temperature profiles in the unstable atmospheric surface layer. *J. Appl. Meteor.*, **9,** 857–861.

Sawford, B. L., and F. M. Guest, 1988: Uniqueness and universality of Lagrangian stochastic models of turbulent dispersion. *Proc. Eighth Symp. on Turbulence and Diffusion,* San Diego, CA, Amer. Meteor. Soc., 96–99.

Smith, F. B., 1957: The diffusion of smoke from a continuous elevated point-source into a turbulent atmosphere. *J. Fluid Mech.*, **2,** 49–76.

Stull, R. B., 1988: *An Introduction to Boundary Layer Meteorology.* Kluwer Academic Publishers, 666 pp.

Thomson, D. J., 1987: Criteria for the selection of stochastic models of particle trajectories in turbulent flows. *J. Fluid Mech.*, **180,** 529–556.

——, 1990: A stochastic model for the motion of particle pairs in isotropic high-Reynolds-number turbulence, and its application to the problem of concentration variance. *J. Fluid Mech.*, **210,** 113–153.

Wilson, J. D., and T. K. Flesch, 1993: Flow boundaries in random-flight dispersion models: Enforcing the well-mixed condition. *J. Appl. Meteor.*, **32,** 1695–1707.

——, G. W. Thurtell, and G. E. Kidd, 1981: Numerical simulation of particle trajectories in inhomogeneous turbulence, III. Comparison of predictions with experimental data for the atmospheric surface-layer. *Bound.-Layer Meteor.*, **21,** 443–463.

——, ——, ——, and E. G. Beauchamp, 1982: Estimation of the rate of gaseous mass transfer from a surface source plot to the atmosphere. *Atmos. Environ.*, **16,** 1861–1867.

——, V. R. Catchpoole, O. T. Denmead, and G. W. Thurtell, 1983: Verification of a simple micrometeorological method for estimating the rate of gaseous mass transfer from the ground to the atmosphere. *Agric. Meteorol.*, **29,** 183–189.

Wyngaard, J. C., O. R. Cote, and K. S. Rao, 1974: Modelling the atmospheric boundary layer. *Adv. Geophys.*, **18A,** 193–211.